

Quantum state transfer in the presence of nonhomogeneous external potentials

Gian Luca Giorgi^{1,2} and Thomas Busch^{1,3}¹*Department of Physics, University College Cork, Cork, Republic of Ireland*²*INRIM, Strada delle Cacce 91, I-10135 Torino, Italy*³*Quantum Systems Unit, Okinawa Institute of Science and Technology, Okinawa 904-0411, Japan*

(Received 20 September 2013; published 5 December 2013)

Heisenberg-type spin models in the limit of a low number of excitations are useful tools to study basic mechanisms in strongly correlated and magnetic systems. Many of these mechanisms can be experimentally tested using ultracold atoms. Here, we discuss the implementation of a quantum state transfer protocol in a tight-binding chain in the presence of an inhomogeneous external potential. We show that it can be used to extend the parameter range in which high-fidelity state transfer can be achieved beyond the well established weak-coupling regime. Among the class of mirror-reflecting potentials that allow for high fidelity quantum state transfer, the harmonic case is especially relevant because it allows us to formulate a proposal for the experimental implementation of the protocol in the context of optical lattices.

DOI: [10.1103/PhysRevA.88.062309](https://doi.org/10.1103/PhysRevA.88.062309)

PACS number(s): 03.67.Hk, 75.10.Pq, 37.10.Jk

I. INTRODUCTION

Single-qubit and two-qubit quantum gates are the basic ingredients for universal quantum computation [1]. If the registers are spatially separated, the required entangling operations can be carried out by either using flying qubits [2] or by quantum state transfer (QST) along a quantum channel, usually modeled as a quantum spin chain in a one-dimensional lattice [3].

Spin chains, however, are a rather mathematical concept, which does not always have a direct realization in a laboratory. Nevertheless, efficient experimental quantum simulation methods to study their properties can be constructed and a common approach uses the internal and external degrees of freedom of trapped particles [4–6]. Another possibility is the use of cold atoms in optical lattices [7,8], where, in particular, the achievement of single-site addressing paves the way to precise initialization and system control [9–12].

The use of long, unmodulated chains has the drawback that almost all the chain modes are involved in the dynamical process. As a consequence, an initially localized wave packet will disperse along the full chain, which strongly affects the efficiency of the QST process. In order to avoid such a dispersive behavior, various proposals have been made. The use of engineered hopping amplitudes between adjacent spins would allow perfect QST independent of the length of the chain [13], but such an implementation would require a high control of the internal structure of the system, while, from the experimental point of view, it is desirable to deal with uniform couplings [14]. The dispersion can also be reduced by encoding the initial state in more than one site [15] or introducing a topological field [16].

An alternative method consists of weakly coupling the two extreme states, the sender and the receiver, to the bulk chain. This allows one to distinguish two different regimes: for very weak coupling, the bulk chain is used as an information bus which is never appreciably populated, and the probability amplitude of finding the excitation at the sender or receiver undergoes an effective Rabi oscillation [17–21]; on the other hand, for nonperturbative end-point couplings, the relevant modes taking part in the quantum state dynamics reside mainly

in the linear zone of the spectrum, thus minimizing the effect of dispersion and allowing QST to occur in the so-called ballistic regime [22–24]. Fast entangling gates can also be built by requiring switchable couplings between qubits and the bus [25]. A review of different QST strategies can be found in Ref. [26].

All the proposals mentioned above share a common feature: the local potential (which, in the language of magnetic systems, corresponds to an external magnetic field) is kept constant along the chain. While this is mathematically convenient, it is by no means always experimentally given. In this work we will show that the presence of a position-dependent potential can indeed help to transfer the quantum state along a chain without making use of any of the techniques listed above. That is, all the spin-spin coupling amplitudes can be kept constant, and we assume no need of any external control. While the requirement of locally modulated spin-spin coupling is something that experimentalists prefer to avoid, spatially modulated potentials naturally arise, for example, in optical lattices due to the Gaussian profile of the laser beams or overlaying magnetic traps [27,28]. The model we study below is therefore suitable for experimental implementation in such a physical context and a schematic is shown in Fig. 1.

The paper is organized as follows. In Sec. II we introduce the spin Hamiltonian model and its basic features; in Sec. III the results are analyzed and we discuss the optimal regimes for high-fidelity QST; in Sec. IV a possible experimental implementation in optical lattices is proposed and, finally, we conclude in Sec. V.

II. MODEL

The Hamiltonian describing a chain of N coupled spins (XX chain) in the presence of a nonhomogeneous external field is given by

$$H = \sum_{n=1}^{N-1} J_n (\sigma_n^x \sigma_{n+1}^x + \sigma_n^y \sigma_{n+1}^y) + \sum_{n=1}^N B_n \sigma_n^z. \quad (1)$$

A relevant property of this Hamiltonian is its symmetry with respect to the operator $S = \sum_l \sigma_l^z$ ($[H, S] = 0$), which implies that the total number of spins up (or down), that is, the total

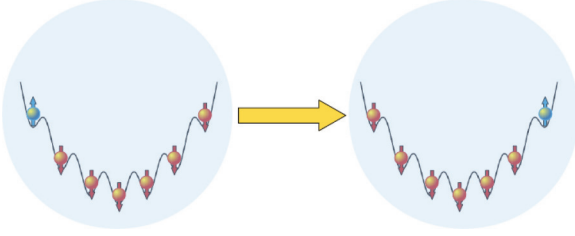


FIG. 1. (Color online) Schematic diagram of the physical implementation of the proposed QST protocol. The spins are arranged in a nonhomogeneous potential obtained by applying a site-dependent external field. The goal of the protocol is to transfer the “up” spin (blue) from the first site to the last one.

magnetization, is conserved. Because of the site dependence of the parameters J_n and B_n , it is generally not possible to diagonalize H , and an analytical solution for the problem cannot be found. On the other hand, as in the following we shall work in the single-particle subspace, the size of the Hilbert space is equal to the number of sites of the chain, and the problem can be easily handled numerically. Let us therefore first consider as an initial state $|\psi\rangle = |1, 0, \dots, 0\rangle \equiv |1\rangle$, which represents one excitation (spin up) on the site 1, while all other spins are down. Because of the conservation of the total magnetization described above and due to the finite intersite coupling amplitudes, the excitation will start hopping between adjacent sites and the state will evolve into $|\psi(t)\rangle = \sum_k c_k(t)|k\rangle$, with $c_1(0) = 1$ and $c_k(0) = 0 \forall k \neq 1$.

The goal of a QST protocol is to let an initial state of the form $|\phi_{\text{in}}\rangle = (\alpha|0\rangle + \beta|1\rangle)|0\rangle^{\otimes N-1}$ dynamically evolve into $|\phi_{\text{out}}\rangle = |0\rangle^{\otimes N-1}(\alpha|0\rangle + \beta|1\rangle)$ for a fixed transfer time. Since $|0\rangle^{\otimes N}$ is an eigenstate of H , it will be sufficient for our purpose to study the conditions under which $|1\rangle|0\rangle^{\otimes N-1}$ evolves into $|0\rangle^{\otimes N-1}|1\rangle$, or, in the language of excitations introduced before, we want to know if there exists a time t^* such that $c_N(t^*) \simeq 1$ and $c_k(t^*) \simeq 0 \forall k \neq N$. In order to get the overall QST fidelity for the system, in principle, one has to average over all the possible initial states (that is, over all the possible combinations of α and β such that $|\alpha|^2 + |\beta|^2 = 1$), but the only relevant parameter is in fact $\langle N|1(t^*)\rangle$.

Let us briefly review the strategy to achieve high-fidelity quantum state transfer based on the weak coupling of the sender and receiver to the bulk chain [$J_1 = J_{N-1} \ll J_n \equiv J$ ($n = 2, 3, \dots, N-2$)] in order to shed light on the underlying physics of the transfer. Considering for the sake of simplicity and without any loss of generality N even, the basic idea of the weak-coupling approach is that the bulk chain behaves just like a bus which is (almost) never excited. This allows the source and the destination to undergo an effective Rabi oscillation (the length of the chain manifests itself in the Rabi frequency), since the two extreme sites behave like a dimer. As discussed in Ref. [19], efficient QST can be reached either by exploiting the resonance of sender and receiver with an isolated level of the channel or by putting them out of resonance. In the first case, an effective three-body oscillation is observed and one of the eigenmodes approximates $|\psi_+\rangle = (|1\rangle + |N\rangle)/\sqrt{2}$ or $|\psi_-\rangle = (|1\rangle - |N\rangle)/\sqrt{2}$, with the sign being determined by the symmetry of the Hamiltonian. In the latter case, there are two eigenmodes close to $|\psi_{\pm}\rangle = (|1\rangle \pm |N\rangle)/\sqrt{2}$. While both

scenarios guarantee high QST fidelity, the QST time turns out to be dramatically reduced in the presence of a resonance. As we will see later in the paper, the external potential can represent a useful tool to move from one regime to the other.

Since dealing with a homogeneous spin-spin coupling amplitude is experimentally very desirable, in the following, we will also look for possible strategies compatible with $J_n \equiv J$, $\forall n$ and use the possibility of having a position-dependent external field as a free parameter. We aim to establish the conditions under which the Rabi-like behavior can be observed independently without resorting to the weak-coupling assumption. Since it is well known that only mirror-symmetric Hamiltonians are suitable for QST [29], we pick an external potential which fulfills this symmetry condition as well as ensuring that $B_n = B_{N-n+1}$. A simple class of external fields which satisfies this criterion is given by

$$B_N = a|n - (N/2)|^p, \quad (2)$$

and two special cases are represented by $p = 0$ and $p = 2$. The first case describes the common, flat potential, while the second one represents the experimentally relevant case of an external harmonic potential [28]. The dynamical evolution of single-particle states in optical lattices with less than 20 sites, under nearest-neighbor spin-spin hopping and in the presence of a harmonic potential, has recently been experimentally observed by Weitenberg *et al.* [11].

The efficiency of a QST transfer protocol is usually estimated by measuring the distance of the real transferred state from the state transferred under optimal conditions using fidelity [30]. As we are interested in studying QST for a broad class of models, calculating the ordinary fidelity would therefore require a huge amount of numerical calculation. Instead, we suggest following a slightly different approach where, instead of focusing on any initial state, we estimate the *transferring ability* of the Hamiltonian by introducing a (sufficient) criterion.

To do this let us consider the set of eigenvectors $|\varepsilon_i\rangle$ of the Hamiltonian H . In the case of ideal transfer, two of them will coincide with $|\psi_+\rangle$ and $|\psi_-\rangle$ and therefore any deviation from the ideal regime can be used as a measure of how much information is lost during the process. To quantify this we define $\mathcal{F} = \max_i \langle 1|\varepsilon_i\rangle - 1/\sqrt{2}$, which we call the *QST drop*. Considering the mirror symmetry of the Hamiltonian, $\mathcal{F} = 0$ implies that $|\psi_+\rangle$ and $|\psi_-\rangle$ are in fact eigenstates. For small values of \mathcal{F} the spectral weight is almost completely absorbed by $|1\rangle$ and $|N\rangle$, while from highly positive or negative values of \mathcal{F} one can deduce the absence of Rabi oscillations due to the dispersive behavior in the chain.

III. RESULTS

The indicator \mathcal{F} introduced before to quantify the QST drop is plotted in Fig. 2 as a function of J_1/J and p , assuming $a = 1/2$ and a chain of $N = 8$ sites with $J_1 = J_{N-1}$ and $J_n \equiv J$ ($n = 2, 3, \dots, N-2$). In any of the figures described in the following, $J \equiv 1$ (together with $\hbar = 1$) is used as energy and inverse time scale. Whilst the details of Fig. 2 will change for different values of N , what is clearly captured here is the transition from the weak-coupling regime to uniform coupling. One can see that for weak external potentials (small p),

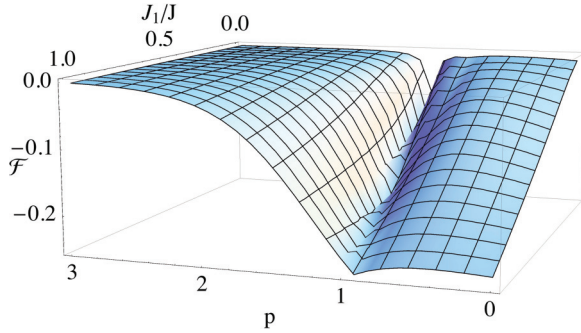


FIG. 2. (Color online) \mathcal{F} as a function of p and the ratio J_1/J . The potential depth is $a = 1/2$. Away from the weak-coupling regime, the presence of the inhomogeneous potential greatly enhances the QST quality.

good fidelities (\mathcal{F} close to 0) can only be achieved using the weak-coupling approach reviewed above and the efficiency drops approximately linear with increasing J_1/J . For p sufficiently strong, however, \mathcal{F} is almost constant and optimal, allowing for the weak-coupling assumption to become unnecessary.

This result can be understood by considering that both weak coupling and strong potential offsets lead to an effective decoupling of the extreme sites from the rest of the chain [31]. The condition for the decoupling to be effective can be obtained, within a perturbation-theory approach, by assuming that the two eigenvalues close to $B_1 = B_N$ are only slightly modified by the presence of the channel. In the weak-coupling limit, the bulk chain (sites from 2 to $N - 1$) forms an energy band, that is, the site index is not a good quantum number and eigenstates correspond to nonlocal modes.

On the other hand, in the case of very strong potentials ($B_n \gg B_{n+1} \forall n > N/2$), each pair of degenerate sites is almost decoupled from all the other pairs and the linear combinations $|\psi_+\rangle$ and $|\psi_-\rangle$ are spontaneously selected in the dynamical process. This result can be understood considering that in the limit of very large p the hopping term of the Hamiltonian only contributes as a perturbation. In the single-site representation, the spectrum is then composed of $N/2$ pairs of degenerate levels, each of them with an energy B_n . By adding the hopping and using a degenerate perturbation-theory approach, one finds that the degeneracy within any of the pairs is removed, and the true eigenstates are close to the linear combinations $(|n\rangle \pm |N - n + 1\rangle)/\sqrt{2}$. Then, in this regime, it is in principle possible to obtain QST between any pair of spins symmetrically displaced with respect to the center of the chain. In the limit of $p \rightarrow \infty$, the potential induces local barriers, giving rise to a transfer mechanism similar to the one proposed by Lorenzo *et al.* in Ref. [32].

Roughly speaking, by assuming $J_1/J \ll 1$, the mode description for the channel fails to give a correct picture when $J^2/|B_2 - B_3| \simeq 1$, that is, when the localization effects of the potential start becoming predominant. For the case depicted in Fig. 2, this rough estimation gives a threshold value $p_{\text{th}} \simeq 1.4$, which is in very good agreement with the observed result. Then, to summarize, high-fidelity QST is achieved either if $p \gtrsim p_{\text{th}}$, irrespective of J_1/J , or if $J_1/J \ll 1$. The dynamics of $|\langle 1|1(t)\rangle|^2$ and $|\langle N|1(t)\rangle|^2$, that is, of the probability to find

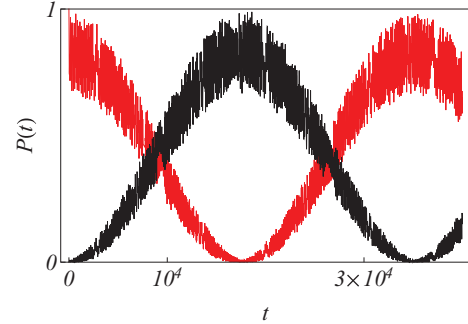


FIG. 3. (Color online) Dynamics of $|\langle 1|1(t)\rangle|^2$ [red (gray)] and $|\langle N|1(t)\rangle|^2$ (black) for a chain of eight sites. The Hamiltonian parameters are $p = 2$, $a = 0.5$, and $J_1/J = 1$. The fast oscillations represent the deviation of the real dynamics from the two-level approximation.

the excitation respectively in the sender and in the receiver station, without relying on the weak-coupling approximation, is depicted in Fig. 3. Channel modes contribute to introduce noise in the transmission process, as witnessed by high-frequency oscillations, but the leading two-mode behavior guarantees high-fidelity QST. Far from the weak-coupling limit, the sharp transition to highly efficient QST in Fig. 2 can be justified, within the perturbation-theory approach described before, by assuming $J^2/|B_1 - B_2| \simeq 1$.

As discussed before, efficient QST in the weak-coupling regime can be obtained either by exploiting the resonance with a single band level or by detuning from all levels comprising the bus. Adding an external potential with adjustable strength or shape can then allow one to drive the system between the first regime and the latter. While the distinction between the two regimes becomes difficult for long chains, where a continuum of states is established, the differences between on and off resonance are clearly observable in short chains, for example, by monitoring the QST time t^* , which is dramatically shorter in the presence of a resonant level. In Fig. 4 (upper panel, red line), the behavior of t^* is plotted as a function of p for a chain of 12 sites. Whenever one of the chain eigenvalues approaches the energy levels of the dimer formed by the sender and the receiver, a faster three-body oscillation takes place causing a reduction of t^* . The number of resonances and their positions therefore depend on the size of the chain. For p large enough, the weak-coupling corrections become negligible since the localizing effect of the potential becomes dominant, as discussed before, and t^* increases monotonically. However, for small values of p , approaching a resonance also implies a degradation of the QST quality (see Fig. 4, upper panel, black line). This can be understood by monitoring how the Hamiltonian eigenvalues change as a function of p . For small p , the two eigenvalues responsible for efficient QST E_+ and E_- , whose corresponding eigenvectors are close to $|\psi_+\rangle = (|1\rangle + |N\rangle)/\sqrt{2}$ and $|\psi_-\rangle = (|1\rangle - |N\rangle)/\sqrt{2}$, are well separated in energy from the rest of the spectrum (Fig. 4, lower panel). There, the continuous line corresponds to the almost degenerate pair E_+ and E_- , while the dotted lines represent the remaining part of the spectrum. As p moves towards the first minimum in Fig. 4, a third eigenvalue becomes closer to E_+ and E_- , and a more efficient three-body

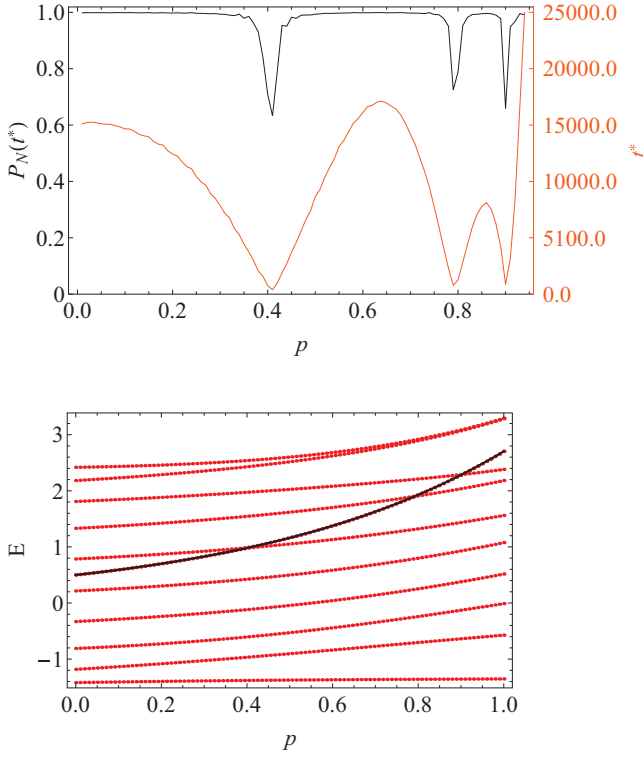


FIG. 4. (Color online) Upper panel: QST time t^* [red (gray) line] as a function of p in the weak-coupling limit ($J_1/J = 10^{-2}$) with $a = 0.5$ for 12 spins. Here, t^* is defined as the first time in which the receiver's site population probability has a relevant maximum (fast oscillations are washed out by averaging the signal over a few periods). The excitation probability at the receiver's site [$P_N(t^*)$] is plotted in black. As explained in the main text, the dips around $p(t^*)$ are caused by the appearance of two oscillation frequencies with unbalanced weights. Lower panel: spectrum of H . The two almost degenerate eigenvalues responsible for high-fidelity QST are the continuous black line, while all the other eigenvalues are in drawn in red (gray).

interaction is established. In this phase, the QST remains very high while t^* decreases. As the three levels get too close to each other, an asymmetric oscillation with two leading frequencies characterized by different weights takes place, whose interference leads to a decrease of the QST fidelity. However, a fine-tuning of p can lead to a substantial reduction of t^* , while keeping the transmission almost perfect.

So far we have described the emergence of localization by tuning p , but obviously the potential depth a can play a similar role. In Fig. 5 we display \mathcal{F} as a function of p and potential depth a , by assuming $J_1/J = 1$ and $N = 8$. As expected, for small a , the external sites can be efficiently isolated from the transmission chain only if p is very large, while smaller values of p are sufficient for larger a . However, increasing a too much amounts to a substantial increase of the QST time. An example is given in Fig. 6, where t^* is studied as a function of a in the harmonic case $p = 2$. We use both the numerical observation of t^* , taken by considering the first time in which $|\langle N|1(t)\rangle|^2$ reaches the arbitrary threshold value of 0.95, and its estimation $t_{\text{est}}^* = \pi |E_+ - E_-|^{-1}$, obtained simply considering a bare model described by the two eigenstates closest to $|\psi_+\rangle$ and $|\psi_-\rangle$. Given the arbitrary value fixed for the numerical

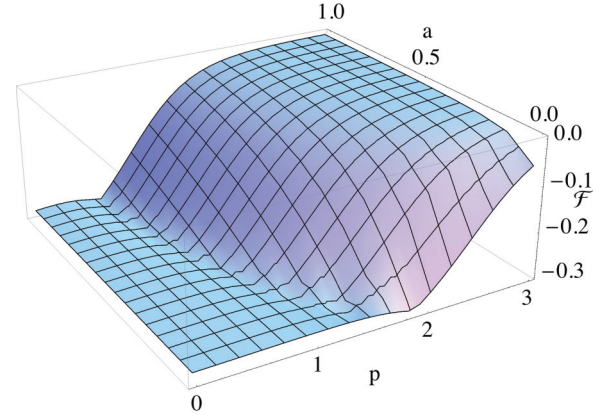


FIG. 5. (Color online) \mathcal{F} as a function of p and a in the constant coupling regime ($J_1 = J$) for $N = 8$.

threshold, the two curves do not assume perfectly identical values. Yet, the qualitative agreement testifying the effective two-level behavior is evident. By comparing Figs. 5 and 6 we deduce that there exists an optimal value of a such that \mathcal{F} is close enough to zero and compatible with a relatively short value of t^* . In the harmonic case, such an optimal value is $a_{\text{opt}} \sim 0.35$.

IV. EXPERIMENTAL PROPOSAL

The nearest-neighbor interaction Hamiltonian model introduced in Eq. (1), in the presence of the harmonic potential described in Eq. (2), was used in Ref. [11] to describe the experimentally observed high-fidelity single-particle tunneling in optical lattices with less than 20 sites. There, coherent evolution in agreement with quantum walk dynamics was observed within a coherence time of a few milliseconds. The experimentally calculated tunneling coupling was $J^{(0)}/\hbar = 940$ Hz in the lower band and the trapping frequency ω_{trap} , which is related to the external potential through $V_{\text{ext}} = m\omega_{\text{trap}}^2 a_{\text{lat}}^2/2$, where m is the atomic mass of ^{87}Rb and $a_{\text{lat}} = 532$ nm is the lattice spacing, was $\omega_{\text{trap}}/(2\pi) = 103$ Hz. Using these numbers, one obtains $V_{\text{ext}}/J^{(0)} \approx 0.1$, which is very close to the optimal value necessary to obtain a high fidelity in a QST protocol (see Fig. 5). Therefore, in the context of atomic lattices, our proposal is only a few technological steps away from being experimentally feasible. Before concluding

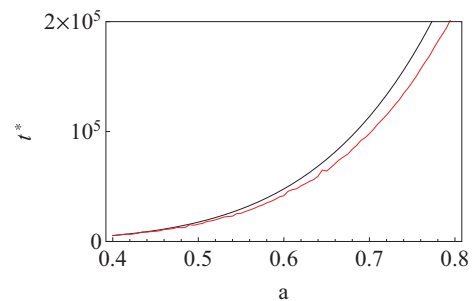


FIG. 6. (Color online) QST time t^* for $J_1 = J$, $p = 2$, and for eight sites. The red (gray) line represents the first time $|\langle N|1(t)\rangle|^2$ reaches the threshold value of 0.95, while the black line is the theoretical estimation $\pi |E_+ - E_-|^{-1}$ of a Rabi oscillation period.

this discussion, we remark that in Ref. [11] coherent spin tunneling was observed in a lattice of 18 sites; however, this is merely a technical and not a fundamental limit for QST implementations.

In the context of ion-trap simulation of spin chains [4], the use of local laser fields can induce an external modulation and any of the values of a and p can in principle be implemented, allowing one to find the optimal conditions for high fidelity and short transfer times.

V. CONCLUSIONS

In conclusion, we have discussed the possibility of implementing a QST protocol in spin chains in the presence of a site-dependent external magnetic field. The field can play a double role. In the weak-coupling limit and for relatively small intensities, it can be used to tune the sender's and the receiver's stations with one of the energy levels of the chain, resulting

in a dramatic reduction of the transfer time of the protocol. Moreover, we have also shown that use of an external field also allows high-fidelity state transfer when traditionally spatially dependent spin-spin coupling would have been necessary.

Among the class of mirror-symmetric potential we have discussed, a prominent role is played by the harmonic modulation, since it is especially suitable for experimental implementation in optical lattices.

ACKNOWLEDGMENTS

This work was supported by Compagnia di San Paolo and by Science Foundation of Ireland under Project No. 10/IN.1/I2979. G.L.G. acknowledges OIST for hospitality. We would like to thank Tony Apollaro, Mauro Paternostro, and Gabriele De Chiara for their comments.

-
- [1] M. A. Nielsen and I. L. Chuang, *Quantum Computation and Quantum Information* (Cambridge University Press, Cambridge, UK, 2000).
- [2] J. I. Cirac, P. Zoller, H. J. Kimble, and H. Mabuchi, *Phys. Rev. Lett.* **78**, 3221 (1997).
- [3] S. Bose, *Phys. Rev. Lett.* **91**, 207901 (2003).
- [4] D. Porras and J. I. Cirac, *Phys. Rev. Lett.* **92**, 207901 (2004).
- [5] X.-L. Deng, D. Porras, and J. I. Cirac, *Phys. Rev. A* **72**, 063407 (2005).
- [6] M. Johanning, A. F. Varon, and C. Wunderlich, *J. Phys. B* **42**, 154009 (2009).
- [7] M. Greiner, O. Mandel, T. Esslinger, T. W. Hänsch, and I. Bloch, *Nature (London)* **415**, 39 (2002).
- [8] L.-M. Duan, E. Demler, and M. D. Lukin, *Phys. Rev. Lett.* **91**, 090402 (2003).
- [9] W. S. Bakr, A. Peng, M. E. Tai, R. Ma, J. Simon, J. I. Gillen, S. Fölling, L. Pollet, and M. Greiner, *Science* **329**, 547 (2010).
- [10] J. F. Sherson, C. Weitenberg, M. Endres, M. Cheneau, I. Bloch, and S. Kuhr, *Nature (London)* **467**, 68 (2010).
- [11] C. Weitenberg, M. Endres, J. F. Sherson, M. Cheneau, P. Schauß, T. Fukuhara, I. Bloch, and S. Kuhr, *Nature (London)* **471**, 319 (2011).
- [12] T. Fukuhara *et al.*, *Nature Phys.* **9**, 235 (2013).
- [13] M. Christandl, N. Datta, A. Ekert, and A. J. Landahl, *Phys. Rev. Lett.* **92**, 187902 (2004).
- [14] C. Ramanathan, P. Cappellaro, L. Viola, and D. G. Cory, *New J. Phys.* **13**, 103015 (2011).
- [15] T. J. Osborne and N. Linden, *Phys. Rev. A* **69**, 052315 (2004).
- [16] S. Paganelli, G. L. Giorgi, and F. de Pasquale, *Fortschr. Phys.* **57**, 1094 (2009).
- [17] A. Wójcik, T. Łuczak, P. Kurzyński, A. Grudka, T. Gdala, and M. Bednarska, *Phys. Rev. A* **72**, 034303 (2005).
- [18] A. Wójcik, T. Łuczak, P. Kurzyński, A. Grudka, T. Gdala, and M. Bednarska, *Phys. Rev. A* **75**, 022330 (2007).
- [19] S. Paganelli, F. de Pasquale, and G. L. Giorgi, *Phys. Rev. A* **74**, 012316 (2006).
- [20] L. Campos Venuti, C. Degli, Esposti Boschi, and M. Roncaglia, *Phys. Rev. Lett.* **99**, 060401 (2007); L. Campos Venuti, S. M. Giampaolo, F. Illuminati, and P. Zanardi, *Phys. Rev. A* **76**, 052328 (2007).
- [21] N. Y. Yao, L. Jiang, A. V. Gorshkov, Z.-X. Gong, A. Zhai, L.-M. Duan, and M. D. Lukin, *Phys. Rev. Lett.* **106**, 040505 (2011).
- [22] L. Bianchi, T. J. G. Apollaro, A. Cuccoli, R. Vaia, and P. Verrucchi, *New J. Phys.* **13**, 123006 (2011).
- [23] T. J. G. Apollaro, L. Bianchi, A. Cuccoli, R. Vaia, and P. Verrucchi, *Phys. Rev. A* **85**, 052319 (2012).
- [24] L. Bianchi and R. Vaia, *J. Math. Phys.* **54**, 043501 (2013).
- [25] L. Bianchi, A. Bayat, P. Verrucchi, and S. Bose, *Phys. Rev. Lett.* **106**, 140501 (2011).
- [26] T. J. G. Apollaro, S. Lorenzo, and F. Plastina, *Int. J. Mod. Phys. B* **27**, 1345035 (2013).
- [27] I. Bloch, *Nature Phys.* **1**, 23 (2005).
- [28] B. Paredes, A. Widera, V. Murg, O. Mandel, S. Fölling, I. Cirac, G. V. Shlyapnikov, T. W. Hänsch, and I. Bloch, *Nature (London)* **429**, 277 (2004).
- [29] M.-H. Yung and S. Bose, *Phys. Rev. A* **71**, 032310 (2005).
- [30] R. Josza, *J. Mod. Opt.* **41**, 2315 (1994).
- [31] S. Paganelli, S. Lorenzo, T. J. G. Apollaro, F. Plastina, and G. L. Giorgi, *Phys. Rev. A* **87**, 062309 (2013).
- [32] S. Lorenzo, T. J. G. Apollaro, A. Sindona, and F. Plastina, *Phys. Rev. A* **87**, 042313 (2013).